Numerical Simulation of the Bubble Dynamics inside an Enclosure Containing Blood under the Influence of Pressure Oscillations

Sara Mashak[1], Mohammad Kazem Moayyedi [1,*], Ramin Kamali Moghadam[2]

[1] CFD, Turbulence and Combustion Research Lab., Department of Mechanical Engineering, University of Qom, Iran
[2] Aerospace Research Institute, Tehran, Iran

ABSTRACT: This study investigates the evolution of bubble shape within a square area filled with blood. The accuracy of the numerical solution is validated using Laplace's problem and the free-rising of the bubble. The analysis is conducted in two dimensions and in a transient manner. The effects of ultrasound waves are applied as a function of pressure on the boundaries of the solution domain. Results show that applying a linearly increasing pressure on the computational domain boundaries causes a reduction in bubble radius. Furthermore, it is observed that assuming the air inside the bubble behaves as an ideal gas, leads to more pronounced changes in bubble radius compared to constant density assumptions. Oscillatory pressure distributions on the external boundaries result in corresponding oscillations in bubble radius. These fluctuations in bubble size could be utilized to exert tension on the walls of blood clots, ultimately aiding in their dissolution. The most intensive bubble size fluctuations occur in the frequency of 1 (MHz). Additionally, the disproportionate changes in bubble radius with pressure variations are attributed to the hysteresis phenomenon.

1- Introduction

Human efforts to cure diseases and illnesses have existed since ancient times. Death and disease due to the formation of blood clots in different organs of the body are among the important cases in medical science. Research has shown that the reason for many strokes, heart attacks, and pulmonary embolism is the presence of blood clots in the vessels. There are different ways to remove blood clots, including the use of clot-dissolving drugs. The disadvantages of this method include the need for long-term treatment. Another method is to use a catheter for local delivery of clot-dissolving agents. Although this method can dissolve the blockage quickly, it is considered an invasive method. Today, microbubbles are widely used in many scientific research and studies as well as in therapeutic cases. One of the applications of small bubbles is to destroy blood clots that cause heart attack, stroke, or even death. Due to the properties of microbubbles, many researches have been done on the application of microbubbles in medical cases.

Researchers investigated methods to expedite clot dissolution through targeted drug delivery using microbubbles. It was found out that, in a rat model of venous thrombosis, residual clot decreased by 67.5% compared to conventional injection. [1]. Tomkins et al. investigated the resilience of platelet-rich clots against thrombolytic treatments, which involve the administration of drugs to dissolve blood clots. Their research revealed that targeted delivery of platelet-rich clots to the main stem of the middle cerebral artery leads to a high occlusion rate and a low rate of spontaneous clot disintegration [2]. Laboratory experiments also show that the use of liposomal bubbles containing Perfluorocarbons accelerates the process of clot dissolution [3]. Hendley et al. used two methods of hemolysis (destruction of red blood cells) and fibrinolysis (dissolution of blood clots naturally) at the same time. The results of their study showed that hemolysis and fibrinolysis methods are equally effective in clot dissolution [4]. Dynamic evaluation of an intravascular bubble was performed by Mashak et al. They observed that when the flow velocity at the inlet boundary is equal to 0.5 m/s along the x-axis, the bubble moves along the vessel from the beginning to the end [5]. The evaluation of the radius changes of a bubble inside a square area containing blood fluid was performed by Kamali et al. in order to check the validity of the numerical solution model, Validation of the Laplace problem and bubble free rising. The problem was analyzed in a two-dimensional and transient manner. The area studied in this simulation was a square area with dimensions of 20 × 20 mm and a bubble inside it with a diameter of 1 mm. It was observed that the radius of the bubble gradually decreases under the influence of this pressure [6]. Gao et al. conducted a comparison between utilizing ultrasound and microbubbles alone versus employing ultrasound,

*Corresponding author's email: moayyedi@qom.ac.ir

microbubbles, and a catheter for clot removal. Their findings revealed that the combined approach significantly enhances cavitation intensity, thereby improving the process of clot dissolution [7]. Exploring a combination approach involving catheter-guided clot dissolution and ultrasound-enhanced clot dissolution with microbubbles demonstrates the safe and efficient improvement of clot dissolution with this combined method. [8]. Additionally, a separate investigation focused on diagnosing acute clots in deep veins. Utilizing Perfluorobutane microbubbles coupled with thrombin-sensitive activator cell-permeable peptides, researchers generated contrast agents that enabled the detection of acute thrombosis via ultrasound imaging [9]. Magnetic microbubble targeting produces an average threefold increase in the rate of clot dissolution [10]. Kim et al. compared the ultrasound dissolution of old clots with the help of low boiling point nano droplets along with phase change with the case of using microbubbles with the same composition, and the result shows the microbubble's capability of creating large cavitation around the clot and subsequently destroying it from the surface of the clot[11]. Dissolution of human blood clots is studied through ultrasound and microbubbles at a pressure of 400 kPa (peak negative pressure), revealing impactful result for clot disintegration[12]. Zhou et al. evaluated ultrasound-assisted clot dissolution for fresh clots with higher cholesterol content. They concluded that no difference is found between clot cholesterol levels and clot dissolution with only ultrasound or tissue plasminogen [13]. Acconcia et al. tested the interaction between microbubbles generated by ultrasound waves and blood clots, revealing that under specific conditions, individual bubbles can breach the clot boundaries, facilitating fluid penetration into it [14]. Pacella et al. treated microemboli formed within the body's capillaries using microbubbles and ultrasound waves, discovering that employing ultrasound waves with an extended pulse length in conjunction with microbubbles can serve as an efficient method for eliminating minuscule clots within the capillaries [15]. Doelare et al. assessed the combined approach of catheter-guided clot dissolution and non-invasive microbubble-ultrasound therapy, demonstrating its reduced risk and treatment duration compared to catheter-guided clot dissolution alone.[16]. Petit et al. evaluated the process of dissolution of blood clots using microbubbles and ultrasound waves, once with drugs that weaken the clot's fibrin structure and again without them. The results of their study showed that the use of fibrin-weakening drugs can improve the performance of the clot dissolution process[17]. The simultaneous use of ultrasound waves and microbubbles along with Urokinase enzyme to destroy blood clots in peripheral arteries was done by Zhu et al. They showed that the rate of clot dissolution accelerates at low frequencies of ultrasound waves [18]. Xie et al. researched the concurrent use of ultrasound waves and microbubbles to dissolve venous blood clots, affirming the efficacy of ultrasound devices coupled with continuous microbubble injection for effectively eliminating such clots [19]. Wang et al. conducted a study on drug transfer using ultrasound waves and micro

bubbles. Their case study was glioma brain tumor. The application of ultrasound waves to the mentioned area led to cavitation and increased drug penetration into the tumor [20]. Zhang et al. aimed to demonstrate a novel vortex ultrasound enabled endovascular thrombolysis method designed for treating cerebral venous sinus thrombosis (CVST). This vortex ultrasound thrombolysis technique potentially presented a new life-saving tool for severe CVST cases that cannot be efficaciously treated using existing therapies [21]. Ostasevicius et al. revealed the influence of low-frequency ultrasound on erythrocyte and platelet aggregation. The obtained results suggested that there are statistically significant variations in blood parameters attributed to ultrasound exposure, particularly when exposed to a high-intensity signal lasting 180 or 90s [22]. Cui et al. developed a new type of ultrasound integrated heart pump assist device (uHPAD) with a pair of ultrasonic transducer rings installed around the pump. Then, in-vivo experiments were performed on sheep to evaluate the efficacy and safety of the novel uHPAD. It was found that the ultrasound assisted thrombolysis with the drug-loaded microbubbles can accelerate the dissolution of the thrombus in the pump, while have no significant negative effect on blood cell components, coagulation-hemolysis system, and the structure and function of main organs. The ultrasound assisted thrombolysis was demonstrated to be a promising method to solve the clinical problem of thrombosis in the HPAD [23]. According to researches, it has been observed that the microbubbles change shape when exposed to ultrasound waves. The pressure caused by the deformation of the micro-bubble can be considered as a factor in removing blockages inside the vessel, including clots.

In this research, a numerical simulation model has been performed to investigate the dynamic behavior of a bubble in a certain volume of blood. The multiphase model based on the Eulerian approach has been used to simulate bubbles in blood. The effects of ultrasound waves have been applied as a function of pressure on the boundaries of the solution domain. The pressure disparity between the interior and exterior of the bubble, influenced by boundary pressures, ultimately drives changes in the bubble's radius. This pressure variation resulting from changes in the bubble's radius can be harnessed to disrupt blood clots within the vessels.

2- Geometry and Boundary Conditions

This study examines changes in air bubble radius within a square area filled with blood fluid. Geometric modeling and mesh generation are conducted using Gambit software, while numerical simulations are performed using ANSYS-FLUENT software. Blood fluid with a density equal to 1110 kg/m³ and a constant viscosity equal to 0.003 kg/m-s is considered as a Newtonian fluid. Since this simulation is two-dimensional, the solution domain is considered a square and the bubble is initiated as a circle inside it. Although the bubble is a three-dimensional shape, because of being placed in a two-dimensional domain, the main forces and effects on the bubble are exerted on it in a two-dimensional field. Therefore, the third dimension and its effects could
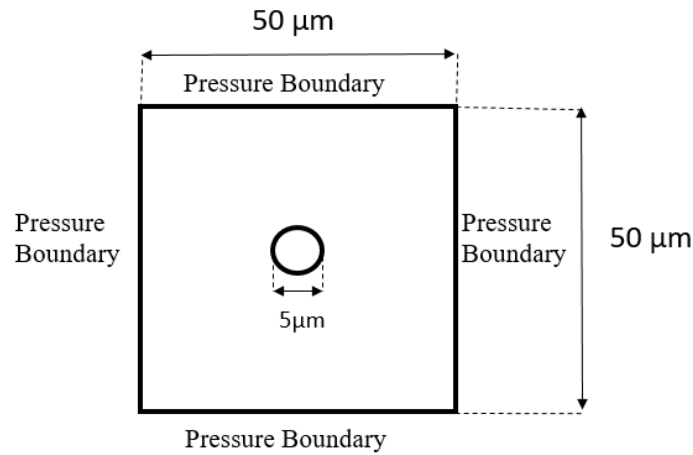
Fig. 1. Schematic of a bubble inside a square-shaped area containing blood
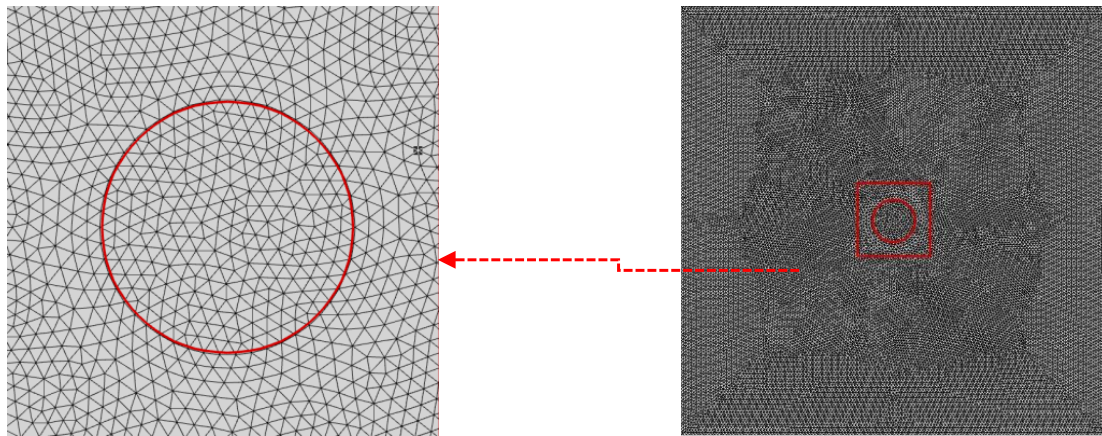
Fig. 2. The Grid containing blood fluid and bubbles in micrometer dimensions

be neglected [24]. Thus, considering the bubble problem in two-dimensional form is an acceptable assumption. But, considering that three-dimensional is closer to the real state. The schematic of the problem is shown in Fig.1.

The forces acting on the bubble shown in this figure include the upward buoyancy force, the surface tension force perpendicular to the bubble surface to the outside, and the force caused by the pressure difference between the blood and the bubble perpendicular to the bubble surface to the inside. The intended area in this study is a square area with dimensions of 50×50 micrometers, and an air bubble with a diameter of 5 micrometers is in its center. Also, an unstructured grid is used according to Fig. 2.

As depicted in Fig. 1, a pressure boundary condition is applied to all four boundaries of the solution domain. This study employs two distinct models to explore how pressure variations along the boundaries impact bubble morphology. In the first model, a linear pressure function according to Eq. (1) and in the second model an oscillating pressure distribution according to Eq. (2) is used as the boundary condition of the pressure on the boundaries of the solution domain. To maintain bubble stability and prevent movement, identical pressure functions are applied to all four boundaries in each model. To implement these pressure functions as boundary conditions, coding is conducted within the user-defined function (UDF) environment. The prescribed functions for the pressure boundary conditions in this study are outlined below:
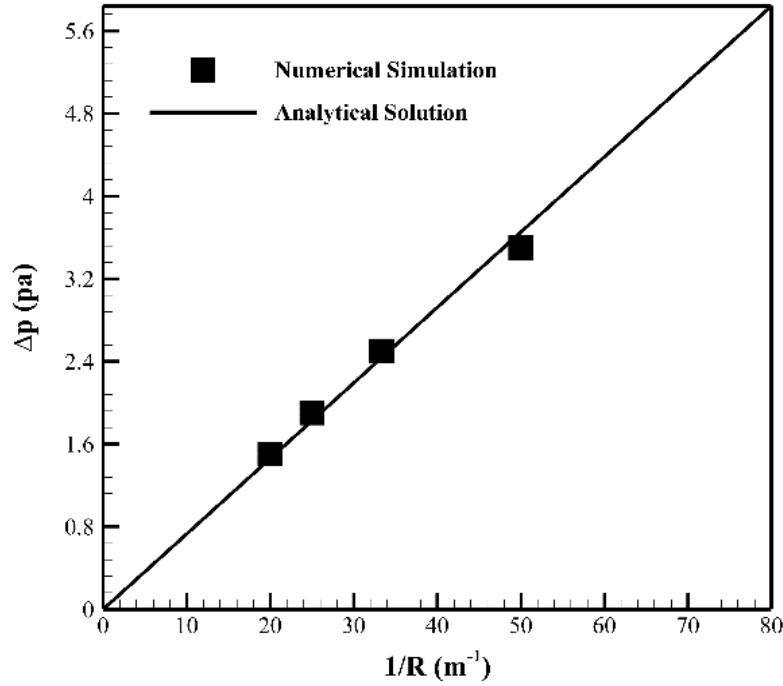
$$p = 2000 + 8t(10^9) \tag{1}$$

Fig. 3. Comparison of the numerical model and analytical method results

$$p = 1.2 \times 101325 \times \cos(2\pi ft) + 130000 \qquad (2)$$

3- Governing Equations

The governing equations of incompressible fluid flow, Navier Stokes equations, include the conservation of mass and momentum. Since this study consists of a bubble inside the blood, it could be considered a multiphase problem. Therefore, the continuity equation for a multiphase model is written as follows:

$$\frac{\partial}{\partial t}(\rho) + \nabla.(\rho\vec{V}) = 0 \qquad (3)$$

$$\rho = \sum R_k \rho_k \qquad (4)$$

where, ρ_k and R_k are density and volume fractions of the kth phase, respectively. Also, ρ and $\vec{V}$ are the density and velocity vector of the multiphase mixture, respectively, and t is time. Since the problem is a multiphase flow, the momentum equation for this type of flow is as follows:

$$\frac{\partial}{\partial t}(\rho\vec{V}) + \nabla.(\rho\vec{V}\vec{V}) = \\ -\nabla.P + \nabla.\left[\mu\ \nabla\vec{V} + \nabla\vec{V}^{T}\ \right] + \rho\vec{g} + \vec{F} \qquad (5)$$

where, ρ, $\vec{V}$, $\vec{F}$ and P are density, velocity vector, Force vector, and pressure for the multiphase flow, respectively. Also, T is the surface stress tensor due to surface tension.

4- Numerical Simulation Method

In this study, the pressure-based solver, and the Volume of Fluid (VOF) method are used to simulate the multiphase flow. The VOF method is used to simulate immiscible two-phase flows and the interface of two fluids. For solving the governing equations, the SIMPLE algorithm, a semi-implicit method for pressure-coupled equations, is employed with second-order accuracy. Geometric modeling and mesh generation are conducted using Gambit software, while numerical simulations are performed using ANSYS-FLUENT software.

In the performed numerical simulation, the surface tension coefficient and the Courant number are considered as 56 N/mm and 0.25, respectively. Moreover, the time step for the simulation is 10^{-10}. Also, the spatial interval between grid points is equally set to be 0.314 μm. The transient
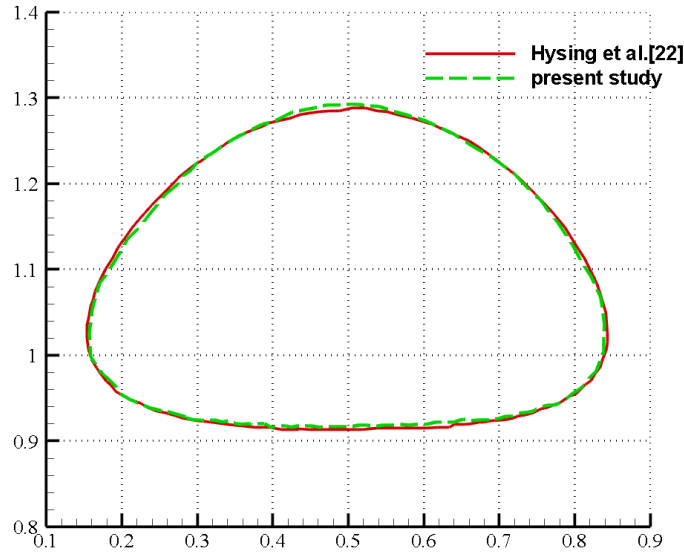
Fig. 4. Comparison of the final shape of the bubble resulting from the numerical solution

formulation method is first-order implicit. The spatial discretization methods for pressure and momentum terms are body force weighted and second-order upwind, respectively. The convergence criteria for the numerical calculations are set as 10^{-3}. Also, the velocity and pressure fields are coupled using the SIMPLE algorithm.

5- Validation of the Numerical Simulation Method

In this study, the Laplace problem and the bubble-free rising problem have been used to validate the numerical model.

5- 1- Laplace Problem

According to Laplace's law, disregarding viscous and gravitational forces while considering surface tension and pressure gradient effects, an air bubble in two-dimensional space will tend to revert to a circular shape if its form deviates from this state. The following analytical relationship is used to calculate the pressure difference between the exterior and interior of the bubble (in two-dimensional space) [25].

$$\Delta p = \frac{\gamma}{R} \tag{6}$$

In the above relation, R indicates the radius of the bubble, and γ represents the coefficient of surface tension. For this purpose, a domain with dimensions of 200×200 mm has been considered. The wall boundary condition has been used for all boundaries. The value of the bubble radius is chosen 20, 30, 40, and 50 mm. According to the explanations, it was finally observed that the shape of the bubble was circular and

according to Fig. 3, the pressure field consists of Eq. (6), and the slope of the line is equal to the value of surface tension.

5- 2- Bubble Free Rising

This validation has been performed based on Hysing et al. [26]. In this research, two dimensionless groups, Reynolds (Re) and Eotvos (Eo) numbers, have been used [26]:

$$\mathrm{Re} = \frac{\rho_1 U_g L}{\mu_1} \tag{7}$$

$$Eo = \frac{\rho_1 U_g^2 L}{\sigma} \tag{8}$$

where ρ_1 liquid phase density, $U_g = \sqrt{g2r_0}$ gravitational speed, $L = 2r_0$ the initial diameter of the bubble, μ_1 the dynamic viscosity of the liquid phase, and σ is the surface tension. Two examples have been examined in Hysing's article. To validate the present numerical work, one of these cases, which includes the numbers $\mathrm{Re} = 35$ and $Eo = 10$, has been selected and the result of the change of the bubble shape has been compared with a similar problem in the article. For this purpose, a solution domain with dimensions of 2 × 1 m has been considered. For the horizontal walls of this range, the non-slip wall boundary condition has been used, and for the vertical walls, the free-slip wall boundary condition has been performed. An air bubble with a diameter of 0.5 meters is positioned such that its center lies 0.5 meters from the bottom side of the solution domain. The parameter

Table 1. The values of the parameters used for free rising of the bubble problem

Parameter	Symbol	Unit	Value
Density of liquid phase	ρ_1	$\dfrac{kg}{m^3}$	1000
Density of air phase	ρ_2	$\dfrac{kg}{m^3}$	100
Dynamic viscosity of liquid phase	μ_1	$\dfrac{kg}{m.s}$	10
Dynamic viscosity of air phase	μ_2	$\dfrac{kg}{m.s}$	1
Gravity acceleration	g	$\dfrac{m}{s^2}$	0.98
Surface tension	σ	$\dfrac{N}{m}$	24.5
Density ratio	$\dfrac{\rho_1}{\rho_2}$	---	10
Dynamic viscosity ratio	$\dfrac{\mu_1}{\mu_2}$	---	10

values utilized are detailed in Table 1 [26].

As observed in Fig. 4, after a period of 3 seconds, the final shape of the bubble obtained from the numerical solution has been matched with acceptable accuracy to the shape of the bubble obtained by Hysing et al.[26].

6- Results and Discussions

As mentioned earlier, based on previous researches, it has been observed that microbubbles change shape when exposed to ultrasound waves. The pressure caused by the deformation of the microbubble could be considered as a factor to remove blockages inside the vessel, including clots. In this study, a part of a blood vessel in the form of a square according to Fig. 1 with dimensions of 50×50 micrometers has been considered, and an air bubble with a diameter of 5 micrometers has been placed inside it. Also, the effects of ultrasound waves have been applied as a pressure function on the pressure inlet boundary condition. In the first step, the effects of ultrasound waves as a linear pressure function applied on the boundaries have been investigated. The amount of this pressure increases over time. The purpose of this work is to investigate the shape change and reduction of the bubble radius, as a result of increasing the pressure on the boundaries and consequently increasing the pressure around the bubble. The simulation results are showcased for two scenarios: the first assumes constant air density, while the second employs the ideal gas law to calculate density. Subsequently,

ultrasound waves are introduced as a fluctuating pressure function through the input pressure boundary condition. The objective of this study is to examine how the bubble's shape responds to surrounding oscillating pressure.

6- 1- Numerical Simulation of Bubble Dynamics due to the Linear Pressure Variation

As described before, an air bubble with a diameter of 5 μm is located in a squared shape domain of 50×50 μm containing blood. A linear pressure function according to Eq. (1) is applied to the boundaries to study the reduction of bubble radius due to the rise of the pressure. Also, this problem has been simulated in two forms of constant air density and ideal gas equation of state.

6- 1- 1- Simulation with Constant Density of Air

In this model, air with constant density is considered as an incompressible fluid. Fig. 5 shows the values of the pressure applied on the external boundaries of the control volume over time. As illustrated in the figure, the pressure applied to the boundaries exhibits a linear increase over time. This trend is attributed to the utilization of Eq. (1) for the pressure term, which represents a linear and ascending relationship. Fig. 6 shows the changes in bubble radius over time during 7.6 microseconds. According to this figure, the radius of the bubble has decreased from the value of 2.5 micrometers at the beginning and reached the value of 2.436 micrometers.
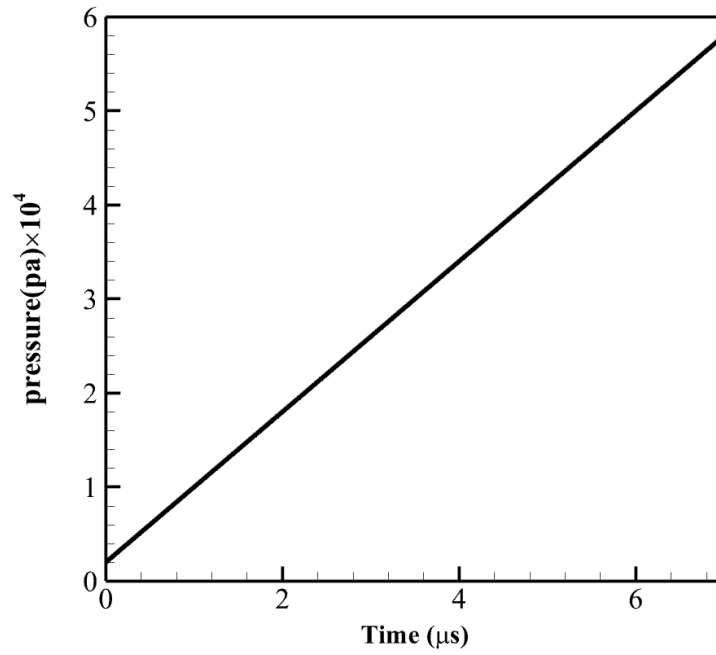
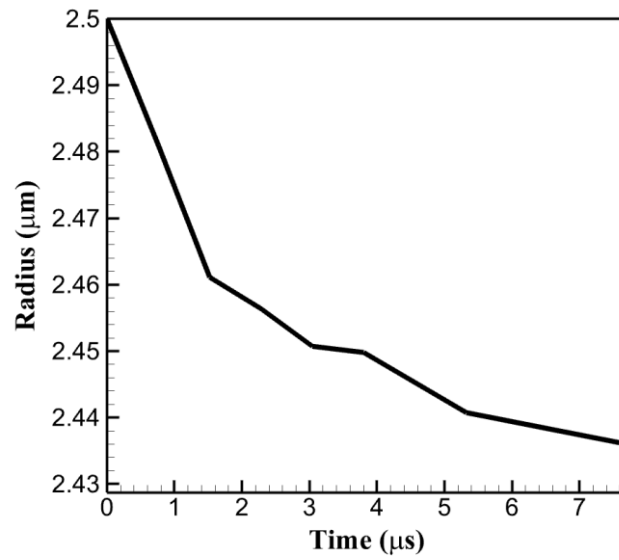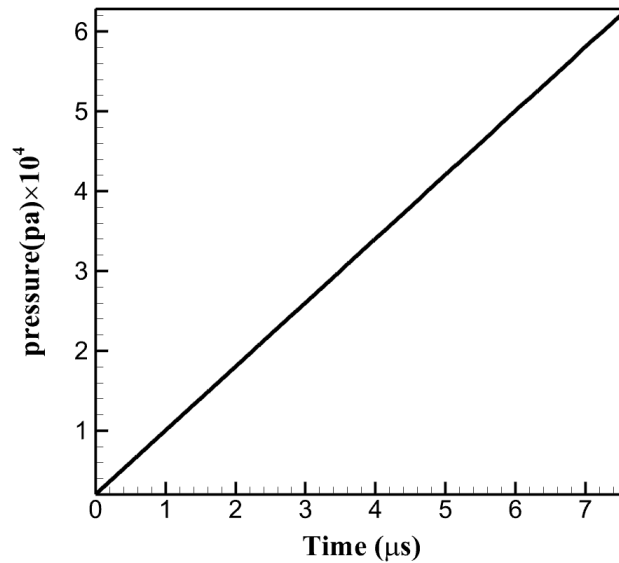**Fig. 5. Pressure variations overtime on the external boundaries of the control volume**

Fig. 6. Bubble radius changes over time

Fig. 7. Pressure variations versus time on the external boundaries of the control volume

The decrease in bubble radius results from the escalation of pressure at the boundaries, leading to an overall rise in pressure surrounding the bubble.

6- 1- 2- Simulation Using Ideal Gas Model for Air

The purpose of studying this model is to increase the effect of pressure changes on the change of bubble radius assuming air compressibility. The important point in the simulation of this model is that the density of the air, which was in a constant state in the previous state, is placed in the ideal gas state in this model. Figs. 7 and 8 show the graph of pressure applied on the boundaries and contours of pressure around the bubble, respectively. By comparing both figures, it is concluded that the amount of pressure on the boundaries and around the bubble has increased over time.

According to Fig. 9, the radius of the bubble has decreased over time because the amount of pressure around the bubble has been increased (Fig. 7). Moreover, when applying identical pressure to a compressible fluid, the volume reduction is significantly greater compared to an incompressible fluid. Consequently, in the second model, the decrease in bubble radius due to increased surrounding pressure is notably more pronounced than in the first model.

### 6- 2- Numerical Simulation of Bubble Dynamics due to the Pressure Oscillation

In this problem, the geometry is similar to the model in the previous test case. Additionally, an oscillating pressure function is applied to the boundaries following Eq. (2). The objective of this research is to explore the variation in bubble radius in response to oscillating pressure alterations. As outlined in section 6.1, it is anticipated that an increase in pressure will lead to a reduction in bubble radius, while a decrease in pressure applied to the boundaries will result in an increase in bubble radius. This modeling has been done by assuming the ideal gas model for air at three frequencies of 5×10^5, 10^6, and 2×10^6. In the first model, the frequency was considered as 10^6 Hz. As the pressure function applied to the boundaries of the control volume transitions from a linear to an oscillatory state, the pressure diagram utilized as an input boundary condition on the domain's boundaries is illustrated in Fig. 10.

Additionally, Fig. 11 displays pressure contours around the bubble at various time points. A comparison between Figs. 10 and 11 reveal that with oscillating pressure applied to the boundaries, the pressure surrounding the bubble also oscillates over time.

Fig. 12 depicts the changes in bubble radius over time. Upon examination of Fig. 12 and Fig. 13, it becomes evident that the fluctuations in bubble radius follow an oscillatory pattern. However, upon comparing the variations in applied pressure on the boundaries with those in bubble radius, it is noted that the changes in bubble radius are not directly proportional to the pressure oscillations. Despite expectations that an increase in boundary pressure should lead to a decrease in bubble radius, and vice versa, this paradox is explained by a phenomenon known as hysteresis. Hysteresis is a phenomenon that shows the dependence of the current state of a system on its previous states. The reason for the name of the loop in the phenomenon of hysteresis is that
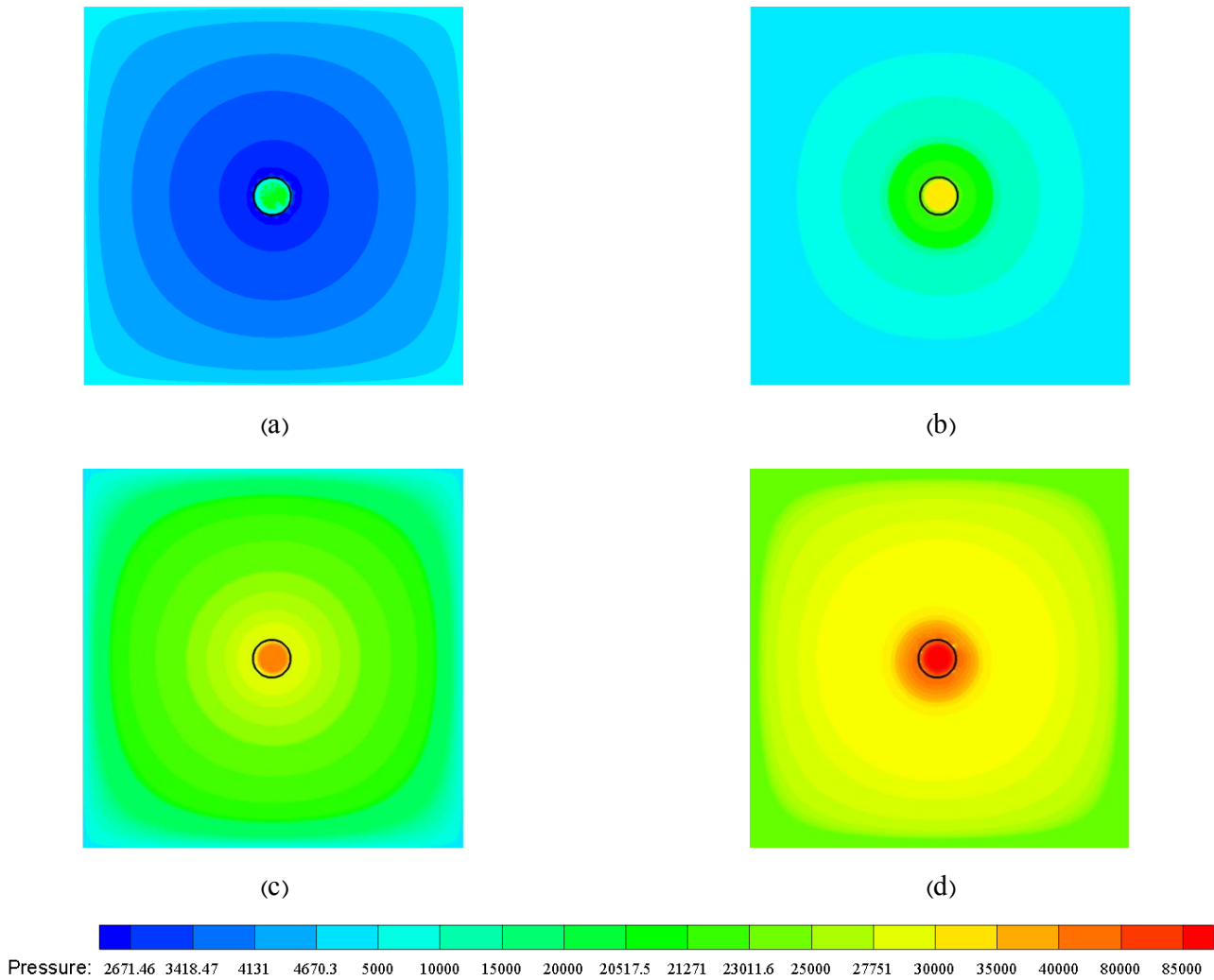
Fig. 8. Pressure changes around the bubble at (a) t = 0.38 µs, (b) t = 0.76 µs, (c) t = 2.28 µs, (d) t= 6.84 µs

two opposite states occur repeatedly, such as the contraction and expansion of a bubble or the loading and unloading of a rubber band. Throughout the continuous contraction and expansion of the bubble, hysteresis behavior is evident. This phenomenon is attributed to gas compressibility, leading to distinct bubble behaviors during contraction and expansion phases. Therefore, it will result in the problem of asymmetry between contraction and expansion. Hysteresis causes the shape of the bubble to be different than expected during the contraction and expansion of the bubble because the bubble does not behave in the same way during the contraction and expansion processes.[27, 28]

As depicted in Fig. 14, the relationship between bubble radius and pressure gradient resembles a ring. Consequently, in light of the explanations provided regarding the hysteresis

phenomenon and Fig. 14, the disparity in radius changes corresponding to pressure alterations can be rationalized by this phenomenon. Figure 15 illustrates the variations in bubble radius over time for a frequency value of 5×10^5 Hz. It is evident from this figure that the changes in bubble radius differ from those observed at a frequency of 10^6. Fig. 16 shows the changes in the bubble radius for the case where the frequency value is twice the value of 10^6. As can be seen in Fig. 17, the bubble radius changes at the frequency of 10^6 Hz are larger than other frequencies. According to this figure, since the amplitude of fluctuations does not have a direct or inverse relationship with the frequency, it could be concluded that the frequency value of 1 MHz is close to the natural frequency of the system.
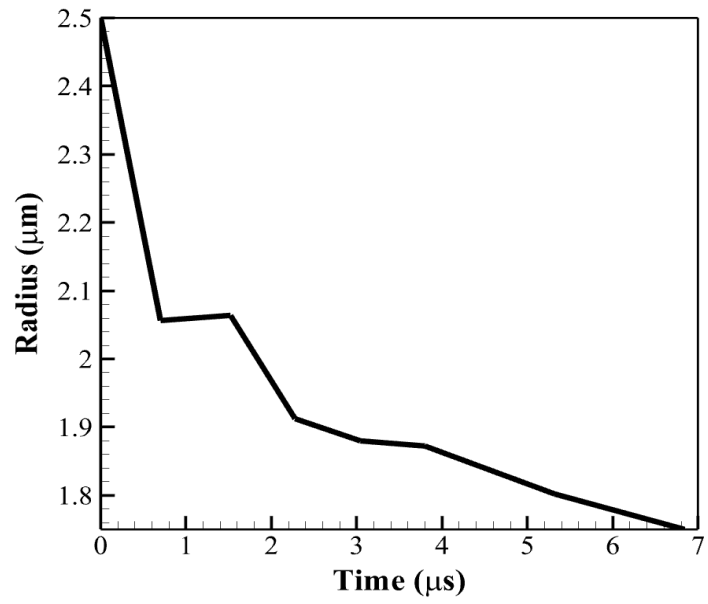
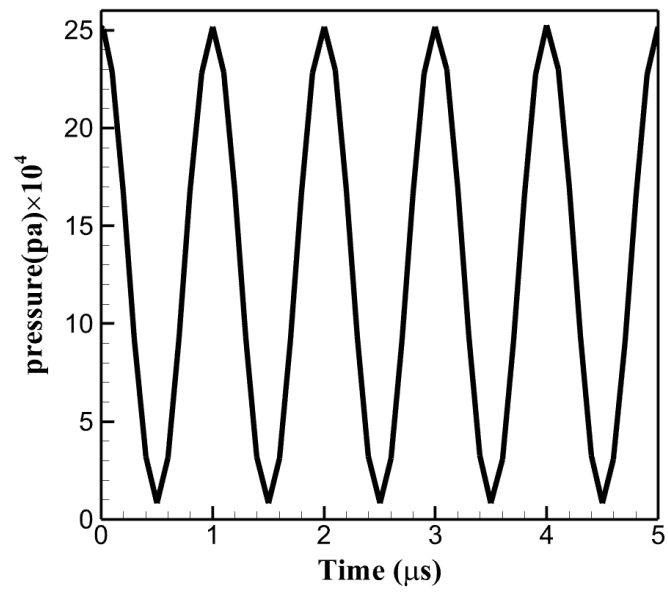**Fig. 9. Bubble radius changes over time**

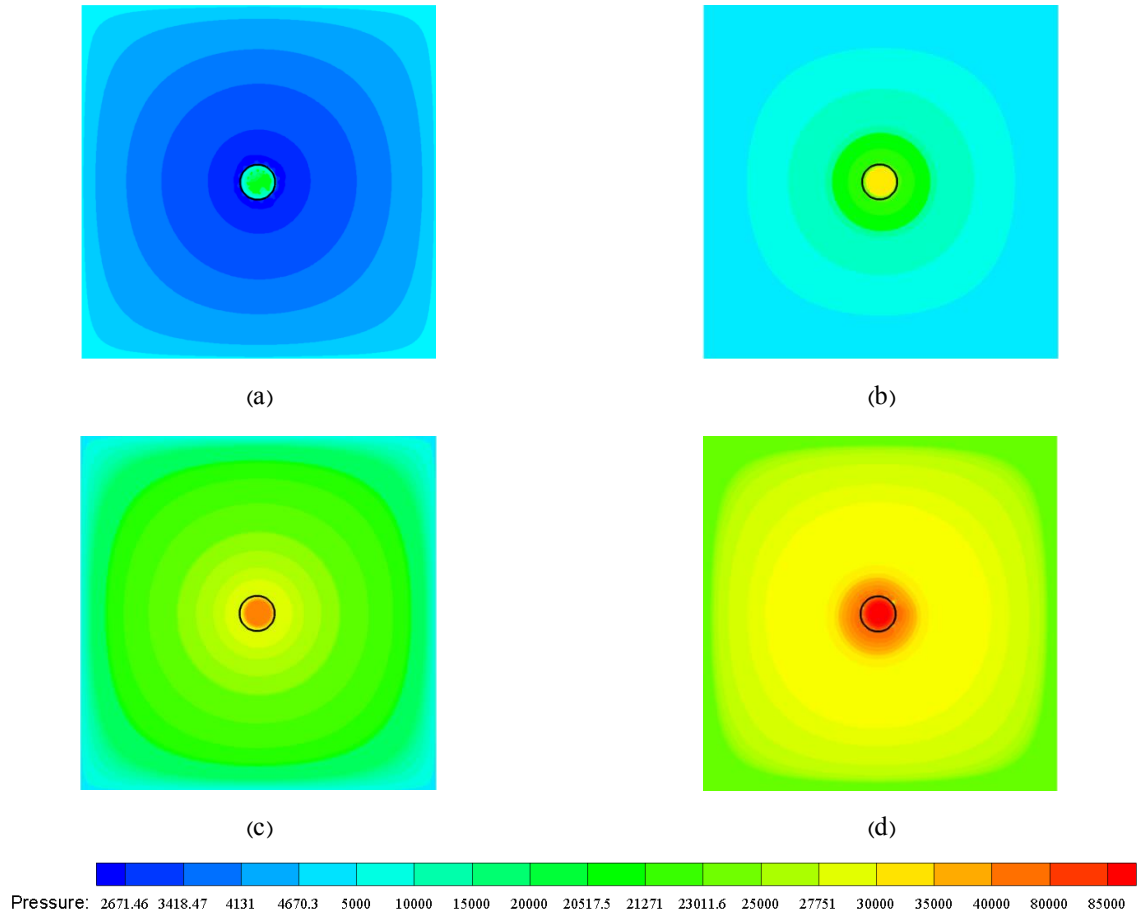**Fig. 10. Pressure variations on the boundaries of the control volume versus time**

Pressure: 2671.46 3418.47 4131 4670.3 5000 10000 15000 20000 20517.5 21271 23011.6 25000 27751 30000 35000 40000 80000 85000

Fig. 11. Pressure changes around the bubble at (a) t =0.02 µs, (b) t = 0.4µs, (c) t = 0.5 µs, (d) t=0.9 µs
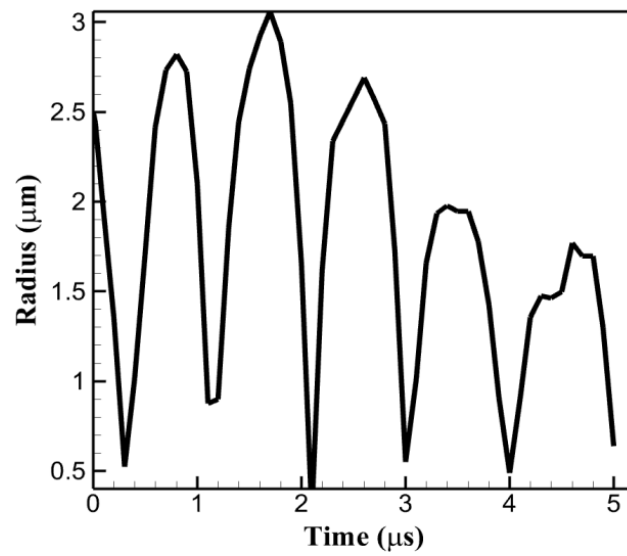
Fig. 12. Bubble radius variations over time
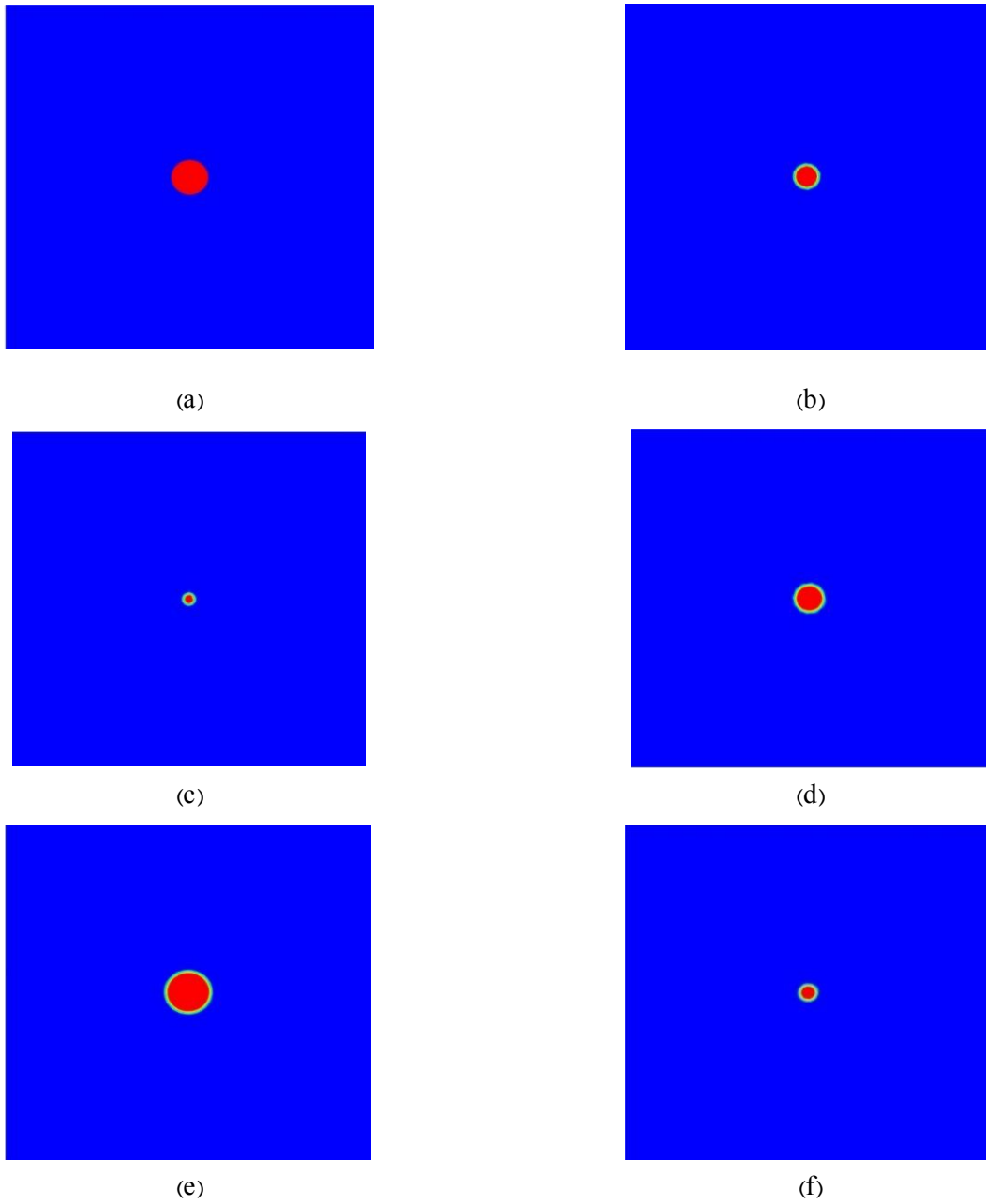
Fig. 13. Variations of bubble radius at (a) t = 0.02 μs, (b) t = 0.2 μs, (c) t = 0.3 μs, (d) t= 0.5 μs, (e) t= 0.8 μs, and (f) t= 1.1 μs
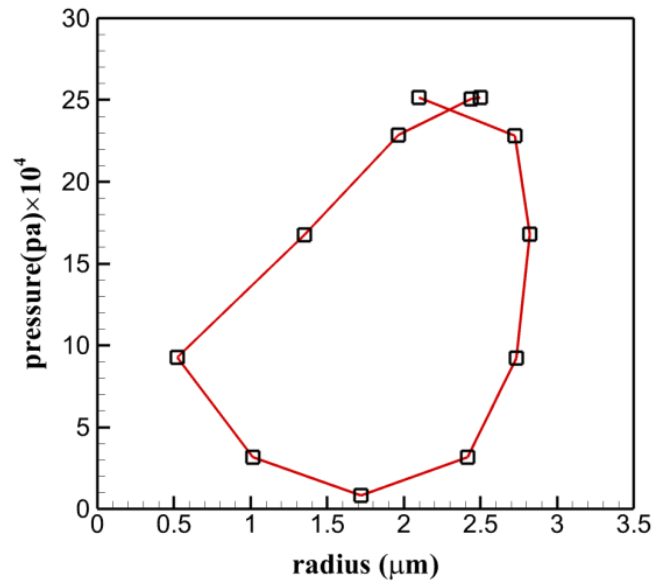
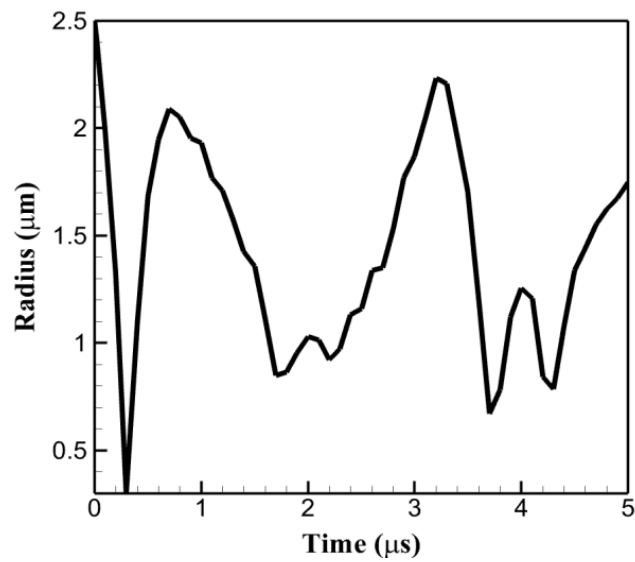**Fig. 14. Variations of Bubble Radius versus Pressure Changes**

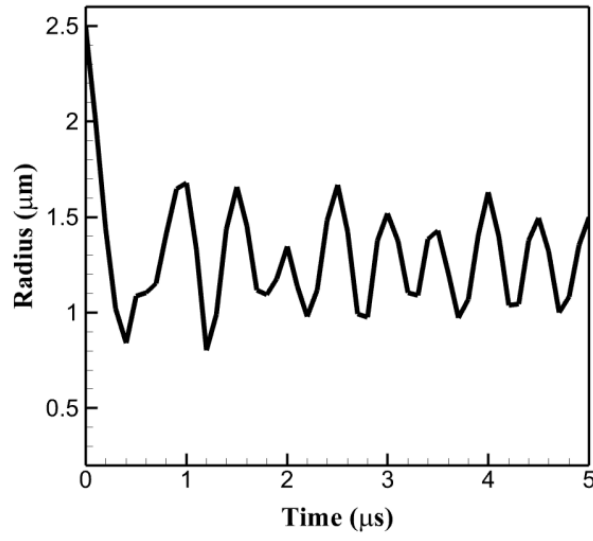**Fig. 15. Bubble radius variations versus time**

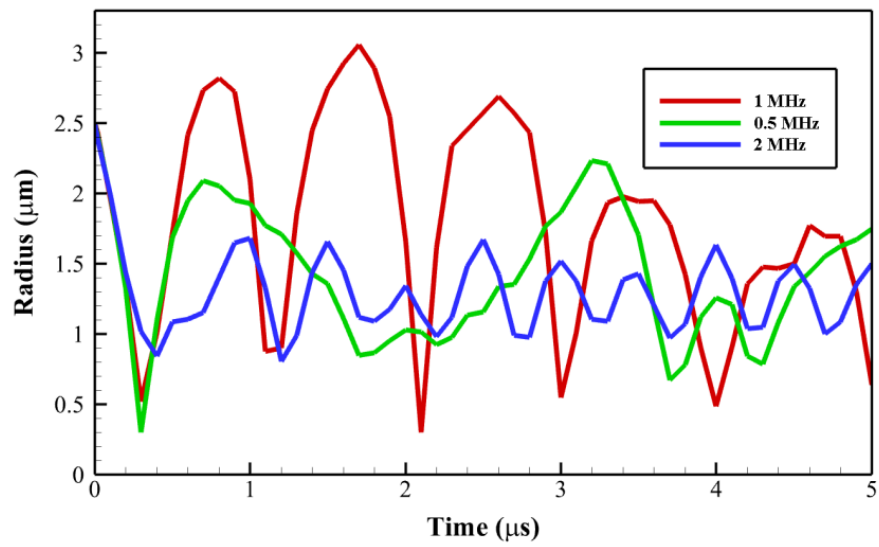**Fig. 16. Bubble radius variations versus time**

Fig. 17. Comparison of bubble radius variation versus time in three different frequencies

7- Conclusion

According to the validation of Laplace and the free rising of the bubble, the results of this study are in acceptable agreement with the benchmark data. In this study, it was concluded that by linear increasing of pressure versus time on the boundaries, the radius of the bubble decreases. It was also observed that when the density of the air is modeled by the ideal gas state equation, the variations of the bubble radius are more significant compared to the case when the density of the air is considered constant. Also, it was concluded that by applying the pressure oscillations on all boundaries of the domain, the radius of the bubble changes in an oscillatory manner. These changes were compared for three different frequencies. The disproportion of fluctuating changes in bubble radius with pressure variations was also justified by using the hysteresis phenomenon. Observations revealed that applying oscillating pressure on the boundaries alters the pressure surrounding the bubble in an oscillatory fashion, leading to fluctuations in bubble size, both decrease and increase. These fluctuations in bubble size could be utilized to exert tension on the walls of blood clots, ultimately aiding in their dissolution. The most intensive bubble size fluctuations occur in the frequency of 1 MHz

References

[1] S. Wang, X. Guo, W. Xiu, Y. Liu, L. Ren, H. Xiao, F. Yang, Y. Gao, C. Xu, L. Wang, Accelerating thrombolysis using a precision and clot-penetrating drug delivery strategy by nanoparticle-shelled microbubbles, Science Advances, 6(31) (2020) eaaz8204.

[2] A.J. Tomkins, N. Schleicher, L. Murtha, M. Kaps, C.R. Levi, M. Nedelmann, N.J. Spratt, Platelet rich clots are resistant to lysis by thrombolytic therapy in a rat model of embolic stroke, Experimental & Translational Stroke Medicine, 7(1) (2015) 2.

[3] K. Hagisawa, T. Nishioka, R. Suzuki, K. Maruyama, B. Takase, M. Ishihara, A. Kurita, N. Yoshimoto, Y. Nishida, K. Iida, H. Luo, R.J. Siegel, Thrombus-targeted perfluorocarbon-containing liposomal bubbles for enhancement of ultrasonic thrombolysis: in vitro and in vivo study, Journal of Thrombosis and Haemostasis, 11(8) (2013) 1565-1573.

[4] S. Hendley, J. Paul, A. Maxwell, K. Haworth, C. Holland, K. Bader, Clot Degradation Under the Action of Histotripsy Bubble Activity and a Lytic Drug, IEEE transactions on ultrasonics, ferroelectrics, and frequency control, PP (2021).

[5] S. Mashak Sh., M.K. Moayyedi, R. Kamali Moghadam, M. Najafi, Numerical simulation of bubble dynamics inside a blood vessel. The 29th annual international conference of the Iranian Mechanical Engineers Association and the 8th conference of the thermal power plants industry, 2021.

[6] R. Kamali Moghadam, M.K. Moayyedi, S. Mashak Sh., M. Najafi, Numerical simulation of the change of bubble radius inside the blood under the influence of linear pressure changes. The 30th annual international conference of the Iranian Mechanical Engineers Association, 2022. Tehran.

[7] S. Gao, Q. Zhu, M. Guo, Y. Gao, X. Dong, Z. Chen, Z. Liu, F. Xie, Ultrasound and Intra-Clot Microbubbles Enhanced Catheter-Directed Thrombolysis in Vitro and in Vivo, Ultrasound in medicine & biology, 43(8) (2017) 1671-1678.

[8] Q. Zhu, G. Dong, Z. Wang, L. Sun, S. Gao, Z. Liu, Intra-clot Microbubble-Enhanced Ultrasound Accelerates Catheter-Directed Thrombolysis for Deep Vein Thrombosis: A Clinical Study, Ultrasound in medicine & biology, 45(9) (2019) 2427-2433.

[9] J. Lux, A.M. Vezeridis, K. Hoyt, S.R. Adams, A.M. Armstrong, S.R. Sirsi, R.F. Mattrey, Thrombin-Activatable Microbubbles as Potential Ultrasound Contrast Agents for the Detection of Acute Thrombosis, ACS Appl Mater Interfaces, 9(43) (2017) 37587-37596.

[10] M. de Saint Victor, L.C. Barnsley, D. Carugo, J. Owen, C.C. Coussios, E. Stride, Sonothrombolysis with Magnetically Targeted Microbubbles, Ultrasound in medicine & biology, 45(5) (2019) 1151-1163.

[11] J. Kim, R.M. DeRuiter, L. Goel, Z. Xu, X. Jiang, P.A. Dayton, A Comparison of Sonothrombolysis in Aged Clots between Low-Boiling-Point Phase-Change Nanodroplets and Microbubbles of the Same Composition, Ultrasound in medicine & biology, 46(11) (2020) 3059-3068.

[12] B. Petit, E. Gaud, D. Colevret, M. Arditi, F. Yan, F. Tranquart, E. Allémann, In Vitro Sonothrombolysis of Human Blood Clots with BR38 Microbubbles, Ultrasound in medicine & biology, 38 (2012) 1222-1233.

[13] Y. Zhou, V.K. Sharma, K.S. Murugappan, A. Ahmad, Clot dissolution is better with ultrasound assisted thrombolysis for fresh clots with higher cholesterol content, AIP Conference Proceedings, 1503(1) (2012) 227-232.

[14] C. Acconcia, B.Y.C. Leung, A. Manjunath, D.E. Goertz, Interactions between Individual Ultrasound-Stimulated Microbubbles and Fibrin Clots, Ultrasound in Medicine and Biology, 40(9) (2014) 2134-2150.

[15] J.J. Pacella, J. Brands, F.G. Schnatz, J.J. Black, X. Chen, F.S. Villanueva, Treatment of Microvascular Micro-embolization Using Microbubbles and Long-Tone-Burst Ultrasound: An inVivo Study, Ultrasound in Medicine and Biology, 41(2) (2015) 456-464.

[16] S.A.N. Doelare, D.M. Jean Pierre, J.H. Nederhoed, S.P.M. Smorenburg, R.J. Lely, V. Jongkind, A.W.J. Hoksbergen, H.P. Ebben, K.K. Yeung, W. Wisselink, B.B. van der Meijs, M.R. Meijerink, A.M. Wiersema, J. Kievit, R.J.P. Musters, J.D. Blankensteijn, O. Kamp, J. Slikkerveer, Microbubbles and Ultrasound Accelerated Thrombolysis for Peripheral Arterial Occlusions: The Outcomes of a Single Arm Phase II Trial, European Journal of Vascular and Endovascular Surgery, 62(3) (2021) 463-468.

[17] B. Petit, F. Yan, P. Bussat, Y. Bohren, E. Gaud, P. Fontana, F. Tranquart, E. Allémann, Fibrin degradation during sonothrombolysis – Effect of ultrasound, microbubbles and tissue plasminogen activator, Journal of Drug Delivery Science and Technology, 25 (2015) 29-35.

[18] Y. Zhu, L. Guan, Y. Mu, Combined Low-Frequency Ultrasound and Urokinase-Containing Microbubbles in Treatment of Femoral Artery Thrombosis in a Rabbit Model, PLOS ONE, 11(12) (2016) e0168909.

[19] F. Xie, J. Lof, C. Everbach, A. He, R.M. Bennett, T. Matsunaga, J. Johanning, T.R. Porter, Treatment of Acute Intravascular Thrombi With Diagnostic Ultrasound and Intravenous Microbubbles, JACC: Cardiovascular Imaging, 2(4) (2009) 511-518.

[20] F. Wang, L. Dong, S. Liang, X. Wei, Y. Wang, L. Chang, K. Guo, H. Wu, Y. Chang, Y. Yin, L. Wang, Y. Shi, F. Yan, N. Li, Ultrasound-triggered drug delivery for glioma therapy through gambogic acid-loaded nanobubble-microbubble complexes, Biomedicine & Pharmacotherapy, 150 (2022) 113042.

[21] B. Zhang, H. Wu, H. Kim, P. Welch, A. Cornett, G. Stocker, R. Nogueira, J. Kim, G. Owens, P. Dayton, Z. Xu, C. Shi, X. Jiang, A Model of High-Speed Endovascular Sonothrombolysis with Vortex Ultrasound-Induced Shear Stress to Treat Cerebral Venous Sinus Thrombosis, Research, 6 (2023).

[22] V. Ostasevicius, A. Paulauskaite-Taraseviciene, V. Lesauskaite, V. Jurenas, V. Tatarunas, E. Stankevicius, A. Tunaityte, M. Venslauskas, L. Kizauskiene, Prediction of changes in blood parameters induced by low-frequency ultrasound, Applied System Innovation, 6(6) (2023) 99.

[23] Y. Cui, X. Zheng, S. Wang, J. Zhou, G. Yue, P. Peng, Q. Li, J. Li, Y. Li, J. Luo, Evaluation on safety and efficacy of ultrasound assisted thrombolysis in a sheep artificial heart pump, Biocybernetics and Biomedical Engineering, 44(2) (2024) 277-285.

[24] Z.Q. Tan, E.H. Ooi, Y.S. Chiew, J.J. Foo, Y.K. Ng, E.T. Ooi, Modelling the dynamics of microbubble undergoing stable and inertial cavitation: Delineating the effects of ultrasound and microbubble parameters on sonothrombolysis, Biocybernetics and Biomedical Engineering, 44(2) (2024) 358-368.

[25] Ghaderi, A., M. Keihani, and M. Nazari, Simulating the process of bubble ascent under electric field using the Boltzmann network method. Mechanical Engineering, Tabriz University, 2019.

[26] S. Hysing, S. Turek, D. Kuzmin, N. Parolini, E. Burman, S. Ganesan, L. Tobiska, Quantitative benchmark computations of two-dimensional bubble dynamics, International Journal for Numerical Methods in Fluids, 60(11) (2009) 1259-1288.

[27] S. Anna, N. Alvarez, L. Walker, A Microtensiometer To Probe the Effect of Radius of Curvature on Surfactant Transport to a Spherical Interface, Langmuir : the ACS journal of surfaces and colloids, 26 (2010) 13310-13319.

[28] V. Chandran Suja, J.M. Frostad, G.G. Fuller, Impact of Compressibility on the Control of Bubble-Pressure Tensiometers, Langmuir : the ACS journal of surfaces and colloids, 32(46) (2016) 12031-12038.